Water Research 204 (2021) 117595

Contents lists available at ScienceDirect

Water Research

journal homepage: www.elsevier.com/locate/watres

Adapting a drinking water treatment technology for arsenic removal to the context of a small, low-income California community

Sara Glade [a], Siva RS Bandaru [a], Mohit Nahata [a], Jay Majmudar [b], Ashok Gadgil [a,*]

[a] Department of Civil and Environmental Engineering, University of California Berkeley, Berkeley, CA, 94720, United States
[b] Department of Chemical and Biomolecular Engineering, University of California Berkeley, Berkeley, CA, 94720, United States

ARTICLE INFO

Keywords:
Drinking water treatment
Low-income communities
Iron electrocoagulation
Arsenic
California

ABSTRACT

Small, low-income, and rural communities across the United States are disproportionately exposed to arsenic contaminated drinking water because existing treatment solutions are too expensive and difficult to operate. This paper describes efforts to overcome some barriers and limitations of conventional iron electrocoagulation (Fe-EC) to enable its use in the rural Californian (U.S.) context. Barriers and limitations of Fe-EC's application in rural California considered in this work include: 1) Frequent labor intensive electrode cleaning is required to overcome rust accumulation, 2) Electrolysis durations are long, reducing throughput for a given system size, and 3) Waste needs compliance with California standards. We report results from an investigation for overcoming these limitations via a field trial on a farm in Allensworth, a small, low-income, rural community in California. Our strategies to overcome each of the above barriers and limitations are respectively, 1) operating the Fe-EC reactor at high current density to result in sustained Fe production, 2) operating at high charge dosage rate with external H_2O_2, and 3) characterization of the arsenic-laden waste, and are discussed further in the paper. Main findings are: (1) Fe-EC removed arsenic consistently below the federal (and state) standard of 10 μg/L, (2) high current density failed to sustain Fe production whereas low current density did not, (3) electrolysis time decreased from $>$ 1 hour to $<$ 2 min with H_2O_2 dosing of 5 mg/L at higher charge dosage rates, (4) dilution of As-sludge is required to comply with State's non-hazardous waste status, and (5) discrepancies were observed between lab and field results in using current density to overcome labor-intensive electrode cleanings. Finally, implications of overcoming limitations to scale-up of Fe-EC in relevant California communities are discussed.

1. Introduction and background

Arsenic occurs naturally in groundwaters around the world, including in many rural, small, and low-income community water systems in the United States (Welch et al., 2000; State Water Resources Control Board, 2015). The Environmental Protection Agency (EPA) Maximum Contaminant Limit (MCL) for arsenic in drinking water is set at 10 μg/L (United States Environmental Protection Agency 2021). Chronic consumption of drinking water exceeding this MCL can lead to adverse health effects, including internal cancers, skin lesions, neuropathy, and developmental impacts (World Health Organization, 2017).

Effective solutions on the market for treating arsenic contaminated water for potable use include coagulation/filtration, adsorption, ion exchange, reverse osmosis, and iron removal (i.e. oxidation/filtration) (Wang et al., 2011). However, most technologies are considered beyond the technical, managerial, financial capacity of small rural California communities facing arsenic contaminated drinking water (State Water Resources Control Board, 2015). As a result, socioeconomically disadvantaged and minoritized populations in California are disproportionately exposed to arsenic contaminated drinking water (Balazs et al., 2012).

Iron electrocoagulation (Fe-EC) is a promising arsenic removal technology and has been investigated widely both in laboratory and field settings to effectively remove arsenic to less than the EPA MCL of 10 μg/L consistently. Fe-EC removes arsenic by capturing it on insoluble Fe(III) (oxyhydr)oxide precipitates produced in the water through the electrically-driven dissolution of iron electrodes (Ratna Kumar et al., 2004; Lakshmanan et al., 2010; Wan et al., 2011; Amrose et al., 2013; van Genuchten et al., 2014b; Delaire et al., 2017; Amrose et al., 2014; Hernandez et al., 2019; Bandaru et al., 2020a). Specifically, Fe(II) ions migrate from the anode into bulk and undergo further oxidation by dissolved oxygen to form Fe(III) (oxyhydr)oxide (Lakshmanan et al.,

* Corresponding author.
E-mail address: ajgadgil@berkeley.edu (A. Gadgil).

https://doi.org/10.1016/j.watres.2021.117595
Received 29 September 2020; Received in revised form 10 August 2021; Accepted 19 August 2021
Available online 24 August 2021

2010). Reactive Fenton-type intermediates (possibly Fe(IV) species) are produced during the oxidation of Fe(II) by dissolved oxygen at circum-netural pH (Hug and Leupin, 2003). These reactive intermediates selectively oxidize As(III) to As(V), which adsorbs rapidly onto Fe(III) (oxyhydr)oxide precipitates (Li et al., 2012, Delaire et al., 2017). The dissolution of iron electrodes in water is called, for brevity, "iron dosing" (Amrose et al., 2014). After iron dosing and adsorption of arsenic on the resulting Fe(III) (oxyhydr)oxides, the arsenic-bearing sludge, mostly comprising Fe(III) precipitates, is separated from the water and arsenic-safe water is produced (Amrose et al., 2014).

Fe-EC's modular design, minimal supply chain (i.e. Fe plates and alum), requiring low-skilled operators (e.g. high school degree or less) has enabled it to be an effective technology to address arsenic contaminated drinking water in resource-poor decentralized communities globally. Recently, Hernandez et al., 2019 reported successful demonstration of a pilot-scale Fe-EC plant (10,000 L/day capacity) at a resource-poor decentralized rural community near Kolkata, India. This plant has been delivering arsenic safe water to the community at a locally affordable price of less than 1 U.S. cent per liter (Hernandez et al., 2019). While Fe-EC has been demonstrated successfully in India, the implementation of Fe-EC in the United States is poorly understood. We conducted this study as a hypothesis-generating (not as a hypothesis testing) effort, although it occasionally has some aspects of the latter. We explored (and report here) limitations to be overcome for implementing Fe-EC as a scalable, affordable, and distributed solution in resource-constrained regions in rural U.S. communities.

2. Approach

In this study, we hypothesized three major barriers and limitations of Fe-EC as implemented in India. These need addressing before Fe-EC can be translated into a locally affordable, community-scale treatment technology for low income regions in the United States. We describe below the approaches taken to overcome these three barriers and limitations (herein barriers and limitations are referred to as limitations).

2.1. Frequent electrode cleaning is required

The steady accumulation of layers of rust on the iron electrodes leads to the steady deterioration of the Faradaic efficiency (ratio between iron measured in the bulk after electrolysis and iron expected theoretically) in Fe-EC systems (Amrose et al., 2014; van Genuchten et al., 2016; Müller et al., 2019). This decline in Faradaic efficiency is problematic because if iron is not released in sufficient amounts in the bulk water, arsenic might not be removed from the water to below its regulated limit (10 μg/L), as intended. In previous work, this issue was resolved by having operators lightly brush the electrode surfaces daily to abrasively remove the top layer of deposited iron rust (Amrose et al., 2014). However, this approach is infeasible for the U.S. context, because of the much higher labor rates for operators ($15-$85/hr in the United States (Colby et al., 2010) vs. ~$1/hr at the Fe-EC plant in India (Gadgil, 2018)). We investigated automated systems for brushing electrode plates for U.S. applications, however, our multiple attempts at such design led to unattractively large increases in capital costs, by more than 50%.

In continuation of our efforts to overcome this problem, we studied varying an operating parameter, current density (current per unit submerged electrode area (mA/cm^2)) over an extended period at 100 liter (L) scale (operated as a batch process) in the field. Charge dosage rate (C/L/min) is also a relevant variable when considering the operation of Fe-EC systems (Amrose et al., 2013). Charge dosage rate can be correlated to current density by changing the current and keeping the electrode surface area the same. Charge dosage rate can be uncorrelated with current density by keeping the current the same while changing the electrode surface area. Recent observations by Müller et al. (2019), suggested that experimenting with a high charge dosage rate (and resultingly high current density) had the potential to address the decline in Faradaic efficiency and growth of surface layer formation (Müller et al., 2019). Using synthetic Bangladesh groundwater (SBGW, defined in the manuscript) and "soft groundwater" (SBGW electrolyte without Ca and Mg), Müller et al. (2019) observed that low charge dosage rate (and therefore low current density (< 1 mA/cm^2)) resulted in a steadily decreasing Faradaic efficiency of total iron over time (60% after 2 months) whereas higher charge dosage rate (and therefore high current density (> 1 mA/cm^2)) resulted in relative high Faradaic efficiency (> 85%) over 2 months of operation. Müller et al. (2019) speculated that at high current densities, high positive charge of the anode and large flux of positively charged Fe^{2+} ions at the anode/electrolyte interface facilitated rapid migration and diffusion of Fe^{2+} ions into the bulk solution instead of accumulating at the anode surface. The soft SBGW electrolyte used in Müller et al. (2019) is very similar to typical groundwater composition found in California Central Valley (e.g. low Ca and Mg concentrations) (Barazesh et al., 2018). Therefore, we hypothesized that operating Fe-EC at high current density (> 1 mA/cm^2) and low charge dosage rate (< 5 C/L/min) would achieve high Faradaic efficiency of total iron in the bulk solution and hence consistent arsenic removal over extended periods of operation. Additionally, we conducted several short-term experiments in the lab at beaker scale that suggested support for this hypothesis, before we conducted the longer term experiments with 100 L reactors in the field. In this study, we investigated if high current density could offer protection against the decline in Faradaic efficiency on a larger scale Fe-EC system (100 L reactor) treating real arsenic contaminated groundwater in the field conditions. We operated two reactors in the field, one at high current density and one at low current density (as control) at similar operating conditions to those reported in Müller et al. (2019).

2.2. Electrolysis times are long in conventional Fe-EC

In contrast to India where the scale of the Fe-EC technology was designed to deliver arsenic-safe water to meet only the drinking water needs, United States regulations require that all the water delivered to the household by public water systems must be of adequate quality for human consumption regardless of its end use (United States Congress, 2019). This requirement increases the volume of water that must be treated and delivered per person per day, from about 2 gallons (approximately 7.6 liters) in the Indian context to about 100 gallons (approximately 378.5 liters) in the United States context. However, Fe-EC treatment cannot be sped up by simply rapidly releasing a larger amount of iron in the water. Previous work has demonstrated that increasing the rate of iron released in the water by increasing the charge dosage rate (CDR) (C/L/min) decreased the efficiency of arsenic removal, because of the competition between Fe(II) and As(III) for the reactive intermediates (Amrose et al., 2013, Li et al., 2012; Delaire et al., 2017). Thus, for a given iron dose, low CDRs (and therefore, long electrolysis times) were found important to achieve complete oxidation of Fe(II) and high efficiency of arsenic removal (Dubrawski et al., 2015; Bandaru et al., 2020b). However, the long-electrolysis times (on the order of hours) increases the operating costs and the physical footprint of the Fe-EC system when delivering increased volumes of water, making the Fe-EC system unattractive and unaffordable for rural communities in California. Operating Fe-EC at high CDRs (> 10 C/L/min) decreases the electrolysis times (to the order of minutes) and can achieve the high flow rates desired for the U.S context at low operating costs. However, the slow kinetics of oxygen dissolution in water requires Fe-EC to operate at low CDRs to achieve complete Fe(II) oxidation and hence efficient arsenic removal for a given charge dose (C/L) (Bandaru et al., 2020b).

To overcome this limitation, we studied use of hydrogen peroxide (H_2O_2) as an external oxidant to the Fe-EC system in the field. The literature has documented the use of H_2O_2 as an external oxidant at beaker scale using Fe salts (Hug and Leupin, 2003). Use of H_2O_2 as an

external oxidant can enhance the kinetics of Fe(II) oxidation 10,000 times compared to kinetics of oxidation with dissolved oxygen, thus facilitating efficient arsenic removal at a high charge dosage rate (Hug and Leupin, 2003; King and Farlow, 2000). Rapid kinetics between H_2O_2 and Fe(II) to achieve efficient arsenic removal at very high charge dosage rates (~1200 C/L/min) or short electrolysis times (~ seconds) has been reported recently with in-situ H_2O_2 generation by an air-diffusion cathode (Bandaru et al., 2020b). The air cathode assisted Fe-EC is a promising alternative to traditional Fe-EC systems to deliver high flow rates at low operating costs. However, the long-term performance of the air-cathode in the air cathode assisted Fe-EC needs further evaluation and could increase the operating costs (e.g., if the cathode fouled irreversibly).

To our knowledge, the use of H_2O_2 as an external oxidant in the Fe-EC system for arsenic removal remains unexplored in the literature, and the field demonstration of this approach is missing altogether in this space. We explored the efficacy of Fe-EC with externally added H_2O_2 as an affordable solution to address arsenic contamination in rural regions in the United States. Specifically, experiments under laboratory conditions necessarily rely on synthetic groundwater matrices. Only field conditions require the technology to have full exposure to exactly all constituents of the groundwater (even those which we might not have thought relevant for the laboratory synthetic groundwater matrix). These might include specific kinds of natural organic matter, conditions of DO, complexation of the contaminant with suspended clay particles, other organic and biological contaminants (bacteria and algae) that might have been missed in the lab.

2.3. Waste needs characterization as per California state standards

In the context of this work, we defined waste characterization as one of the necessary pieces of knowledge needed for ensuring ability to use the Fe-EC system. This characterization will determine if the arsenic-laden waste generated from the Fe-EC system can pass the two specific tests defined in section to receive regulatory approval for practical implementation of the technology. Lack of knowledge about the sludge is a barrier to use of the technology – it is not a limitation of the technology.

Fe-EC produces an arsenic-laden iron sludge as a waste by-product that must be managed appropriately (Amrose et al., 2014). Two measurements, Total Threshold Limit Concentration (TTLC) and Soluble Threshold Limit Concentration (STLC), are required per Californian regulations to determine the nature of the waste (e.g. hazardous, non-hazardous) and resulting waste management practices needed for scale-up (e.g. landfill disposal) (California Code of Regulations, 2021). TTLC measures the solubilized, extractable, and non-extractable concentrations (i.e. total arsenic), and STLC measures the solubilized and extractable concentrations. The TTLC standard for arsenic is 500 mg/kg and the STLC standard for arsenic is 5 mg/L (California Code of Regulations, 2021). Until now, Fe-EC sludge produced from arsenic-removal process had not been characterized per either standard.

To overcome this knowledge gap, TTLC and STLC values of sludge generated in the field were measured in a third party California Water Boards-certified lab (Enthalpy Analytical at Berkeley, California).

3. Materials and methods

We conducted month-long field testing of a 100 L Fe-EC system in batch mode on a private farm impacted by arsenic contaminated groundwater in Allensworth, California. Allensworth is a small, low-income, rural community in California with a history of struggling with arsenic-contaminated drinking water (State Water Resources Control Board, 2013). The groundwater at the farm had 153 ± 29.1 μg/L of arsenic (nearly 15 times the EPA Maximum Contaminant Level of 10 μg/L for arsenic in the drinking water). Most California wells with arsenic contamination have concentrations that are much lower (< 90 μg/L) (State Water Resources Control Board 2021). The groundwater is pumped directly into the reactors without any pretreatment to understand Fe-EC performance at removing arsenic under realistic operating conditions. We operated two Fe-EC reactors (100 L) in the field in batch mode, one at high current density and one at low current density (as control) at similar operating conditions to those reported in Müller et al. (2019). The location thus allowed testing Fe-EC's performance in a groundwater condition in the context of rural California.

3.1. Chemical analysis and other measurements

Potassium and sodium concentrations were measured using Inductively Coupled Plasma Mass Spectrometry (ICP-MS) (EPA Method 6020). Total iron, silica, phosphorus, magnesium, and calcium were measured using Inductively Coupled Plasma - Optical Emission Spectrometer (ICP-OES). Total arsenic was measured using either ICP-MS or ICP-OES depending on availability of the instruments to the researchers. ICP-MS, ICP-OES, and ion chromatography samples were acidified prior to measurement by adding 1 mL of 1.1 M HCl to a 5 mL sample. Arsenic samples were filtered with a 0.45 μm filter prior to acidification. Chloride, sulfate, and nitrate were measured by ion chromatography (EPA Method 300.0). Alkalinity was measured by titration (SM2320B). Natural organic matter (NOM) was measured through total organic carbon (TOC) using method SM310c. pH, DO, and conductivity were measured in the field using electrode probes (Orion 5 STAR (Thermo Scientific)). Turbidity was measured in the field using a portable turbidity meter (Orion™ AQ4500 Turbidimeter). The concentration of H_2O_2 was measured in the field using a portable spectrophotometer (Hach DR/2400 h) with titanium(IV) oxysulfate solution (Sigma Aldrich) at wavelength 405 nm.

The mass of the iron electrodes before and after the field trial was measured using an electronic scale.

Air temperature was recorded in the field using a thermometer, and water temperature using a multiparameter portable meter (Orion 5 STAR (Thermo Scientific)).

DC power supplies (B&K Precision 1687B, 1688B, 9115) were used to supply desired current for electrolysis. Power supplies were operated in constant current mode at the desired current, and the resulting voltage was recorded in the field near the start and end of electrolysis. Interface potentials near the reactor electrodes were measured in the field using an Ag/AgCl (3M NaCl) reference electrode (BASI) by placing it very close (0.2 cm to 0.5 cm) to the iron electrodes. The potential difference between the reference electrodes and the iron electrode was measured with a multimeter (Fluke 87V) and this value was reported as an interface potential of the electrodes. We assumed a negligible ohmic voltage drop between the reference electrode and iron electrode.

The uncertainty of all measurements reported in this work are shown in parentheses of respective instrument or technique: ICP-MS (±0.1 μg/L) when measuring As, ICP-OES (±0.1 mg/L when measuring Fe, Ca, Mg, Si and P; ±10 μg/L when measuring As), pH (±0.002), DO (±0.2 mg/L), conductivity (±0.5%), thermometer (± 0.1 °C) when measuring water temperature, turbidity (±3 %), titanium(IV) oxysulfate method (±0.5 mg/L) when measuring H_2O_2, electronic scale (±0.01 grams) and voltmeter (±0.1 volts).

3.2. Beaker-scale experiments

Beaker scale (electrolyte volume = 0.2 L) Fe-EC experiments were conducted in the lab at low (0.5 mA/cm^2) and high current density (10 mA/cm^2) using the groundwater collected from the field site. The main objective of these short-term experiments (16 batches) was to investigate the hypothesis that high Faradaic efficiency (> 85 %) of total iron can be achieved when Fe-EC operated at high current density (> 1 mA/cm^2) and low charge dosage rate (< 5 C/L/min) over long-periods of operation. The charge dosage rate was kept constant at 3.1 C/L/min at both current densities and the electrolyte was stirred continuously using

a magnetic stir bar. After delivering the desired dose of 200-300 C/L, samples for total iron were collected and acidified immediately with 1.1 M HCl for ICP-OES analysis. Electrodes were pulled out of the reactor gently, and iron dosed groundwater was replaced with new groundwater in the beaker. Every day up to three experiments were performed at each current density and a total of 16 experiments were completed in 2 weeks at these operating conditions. The electrodes were left to dry overnight and were not cleaned in between the experiments. Electrodes were not cleaned between batches. Batches 1-6 were conducted at approximately 196 C/L and batches 7-16 were conducted at approximately 300 C/L. The operating parameters of these experiments were summarized in SI Table S1.

3.3. Reactors and processes

Pilot scale experiments were conducted to understand the performance of Fe-EC at treating arsenic contaminated groundwater over a long period of time (~ month). The objective of these experiments was similar to the batch experiments described in Section 3.2. Specifically, the purpose was to understand if high Faradaic efficiency of total iron can be achieved in a scaled-up Fe-EC system (100 L reactor volume) operating at high current density (10 mA/cm^2) and low charge dosage rate (3.5 C/L/min) over long-term operation in the field. These experiments were expected to address the frequent electrode cleaning limitation described in Section 2.1.

Two Fe-EC reactors (electrolyte volume =100 L) were constructed at the University of California, Berkeley, and transported to the field site in Allensworth, CA. These reactors were designed to operate at low current density and high current density by changing the electrode surface area (and therefore number of electrodes) while keeping the reactor volume and charge dosage rate the same. Herein, we refer to these reactors as low- and high-current density reactors. The change in shape of the Fe-EC reactors (rectangular for low current density reactor and circular for high current density reactor) do not influence the mixing conditions or the arsenic removal chemistry because electrolyte mixing is achieved by continuously recirculating the electrolyte using a submersible pump during the electrolysis. Similar mixing configuration has been implemented in the published work on Fe-EC systems in the field (Amrose et al., 2014; Hernandez et al., 2019).

The reactors had different number of plates (12 vs 2) to accommodate the low and high current densities while supplying the same current to each of the two reactors. Thus, two designs accommodated the difference in electrode surface areas (as shown in Fig. 1). Note that since both designs held the same water volume, and deployed the same current, they both delivered identical charge dosage rate, but with different current densities on their electrode surfaces. On the low current density reactor, each of the electrode plates was labeled 1 through 12, and the face of each plate was labeled either F (for front) or B (for back). The inter-electrode distance was 2 cm.

During electrolysis, water was aerated using a pipe with holes to jet the water downward through the air. Water was recirculated using a submersible pump (124 watts) through the reactor to replenish dissolved oxygen and ensure mixing. When used, H_2O_2 was added to the solution right above the submersible pump in the reactors (Fig. 1A, submersible pump) to ensure uniform distribution of H_2O_2 throughout the reactor by recirculation. After electrolysis, water with iron-oxide particles was fed to a settling tank (settling process will be described later). Industrial grade non-ferric alum ($(Al_2(SO_4)_3 \bullet 18\ H_2O$) was added to aid in the settling process. Alum stock solution was made to the concentration of 5000 mg/L (as Al). An alum dose of 2.5 to 7.5 mg/L as Al was investigated based on the published literature during the initial testing (data not shown for brevity). We found that the alum dose of 7.5 mg/L as Al resulted in lowest turbidity after 1 minute rapid mixing (~600-800 rpm), 20 minute slow mixing (~20-40 rpm) and 2 hours of settling. The alum dose and parameters for rapid and slow mixing were selected based on the published literature (Amrose et al., 2014; Hernandez et al., 2019).

3.4. Field operation

The reactors were each operated typically one to two times per day for five days per week for four weeks in June 2019. Table 1 presents the operating conditions for this part of the field trial. The dose and charge dosage rate were target values. The current was measured. The current density was calculated.

Batches 1-2 were test runs used to ensure the basic system components (e.g. pumps, power supplies) were operating as designed.

Batches 3-5 were designed to determine the minimum dose of iron required to remove arsenic to less than 10 μg/L. This was achieved by measuring arsenic removal in the field over a wide range of doses (0-400

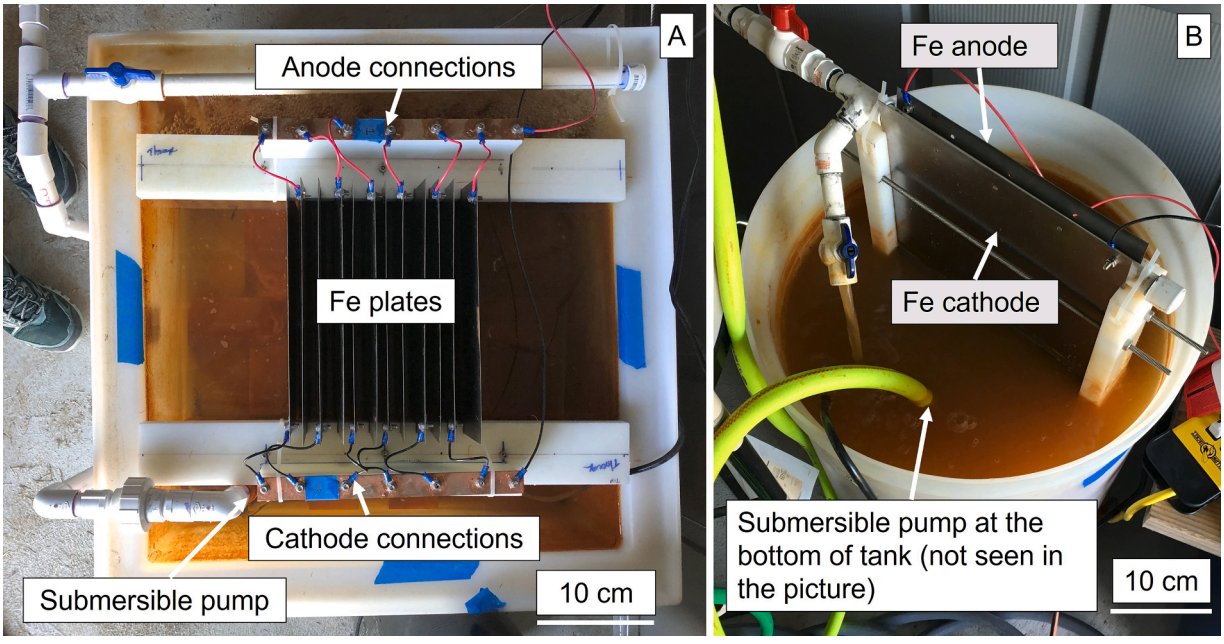

Fig. 1. Digital images of the Fe-EC reactors (A- low current density reactor, B- high current density reactor).

Table 1
Field-Experimental conditions (June 2019).

Batch number	Purpose	Dose (C/L)	Current (A)	Charge Dosage Rate (C/L/min)	Current Density (mA/cm^2)
1-2	Test runs	429, 572	8.3	5.0	0.89 (low) 15.32 (high)
3-5	Minimum dose experiments	400	5.8	3.5	0.62 (low) 10.7 (high)
6-13	Long term test of performance	150	5.8	3.5	0.62 (low) 10.7 (high)
14-37	Long term test of performance	150	3.5	2.1	0.37 (low) 6.5 (high)

Experiments for batches 1-9 were conducted during week 1, batches 10-18 during week 2, batches 19-27 during week 3, and batches 28-37 during week 4 in June 2019. The surface area to volume (A/V, cm^2/L) for the low current density and high current density reactors are 90.0 and 5.4 respectively.

C/L) (0 C/L referring to raw water without treatment or particle separation). Data at 0, 50, 100 C/L were duplicate measurements and everything else was triplicated.

Batches 6-37 were operated at the above-determined minimum dose to examine the long-term performance of the Fe-EC system with respect to arsenic removal, Faradaic efficiency of total iron, and energy consumption.

H_2O_2 experiments were conducted using the field trial setup and low current density reactor in July 2019, and explored the influence of H_2O_2 concentration and charge dosage rate on arsenic removal performance. New electrode plates were used in the low current density reactor for H_2O_2 experiments. Table 2 presents the operating conditions for this part of the field trial. The dosage rate in the July field experiments was selected to be nearly an order of magnitude higher than the dosage rate in the June field experiments to investigate arsenic removal with a shorter electrolysis time.

Raw water samples were collected once per day from the groundwater source. Water pumped from wells entered a tank, where it was pumped out into a hose that entered either reactor. Before conducting experiments each day, we let the water leaving the tank flush for 5 minutes. Pre- and post-electrolysis samples were collected from the electrolysis tanks at the end of each experiment. Samples were collected while the recirculation pump was running to prevent any settling of the suspension leading to non-uniform concentrations of total iron in the solution. The solution pH, DO, and conductivity were measured in one set of samples right after the collection. Samples for total concentrations of the solution species were acidified immediately with 1.1 M HCl. Samples for dissolved concentrations of the species were filtered using 0.45 μm nylon syringe filters and the filtrate was acidified immediately with 1.1 M HCl. We filtered the samples to understand the degree of arsenic removal possible, if the particle separation was fully effective. It was important to separate the arsenic removal results from those of the particle separation approaches tested. Similarly, post-settling samples and post-filtration samples for the total concentrations of solution species and dissolved concentrations of the solution species were collected from the settling tank and at the outlet hose when half the settling tank was drained. Particle separation approaches investigated in this study are presented in the supporting information (Section S2). We did not explore particle separation exhaustively to include this section in the main manuscript. Hence these findings are presented in SI so that other researchers may find them useful in their future work.

Table 2
Field-Experimental conditions of tests with H_2O_2 addition (July 2019).

H_2O_2 concentration in the raw water (mg/L)	Charge Dose (C/L)	Current (A)	Charge Dosage Rate (C/L/min)	Current Density (mA/cm^2)
0, 5, 26	50, 100, 150	50	30	5.6

Single test was performed with 0 mg/L H_2O_2. Duplicate tests were performed with 5 mg/L and 26 mg/L H_2O_2.

3.5. Characterizing sludge

Wet sludge collected from the field was dried in a lab oven at approximately 75°C until water evaporated after the field trial was complete. The drying time was not accurately recorded but it was around a few (3-4) days. STLC and TTLC measurements of the dried sludge were conducted by a third party, California Water Boards-certified lab (Enthalpy Analytical at Berkeley, California). TTLC was done using the method EPA 6020, ICP/MS. STLC was done using WET/EPA 6010B.

4. Results and discussion

4.1. Raw water composition and determining minimum dose

4.1.1. Raw water composition

Conductivity varied greatly over the duration of the field trial, as shown in SI Figure S1, and indicated by the large standard deviation in Table 3. Broadly, the water conductivity was high (4585 μS/cm ± 790 μS/cm) in the first quarter and last quarter portions of the field trial (batches 1-9, and 27-37), and lower (441.9 μS/cm ± 209.9 μS/cm) in batches 10-26. As a result, in several figures we have demarcated these distinct conductivity regimes with vertical lines. Table 3 presents the raw water composition separated into low and high conductivity periods. Table S2 presents the average and standard deviation of the raw water composition throughout the duration of the field trial. We do not know the cause of the conductivity changes; however, we suspect that the variability of pumping on the farm might be a factor. The upper limit allowed in California for chloride and sulfate is 500 mg/L (State Water Resources Control Board, 2018). On average, the chloride and sulfate concentration in the raw water is much higher, and thus would need to be removed in addition to arsenic to provide this water for drinking purposes. TOC was not detected in any sample measured.

4.1.2. Experiments to determine minimum dose

Fig. 2 presents the average arsenic concentration after electrolysis during batches 3-5 at low current density and high current density operation. Dissolved arsenic in the filtered samples decreased from an initial concentration of 185 μg/L to a concentration of 0.2 μg/L as charge dosage increased from 0 to 400 C/L. Dissolved arsenic in the filtered samples decreased to below 10 μg/L at charge dose of 100 C/L or greater. The arsenic removal was similar across the low and high current density reactors, which were supplied with the same current (5.8 A), had the same volume (100L) and therefore the same dosage rates. This is consistent with the earlier reported finding that arsenic removal is more strongly influenced by charge dosage rate than the current density (e.g., Amrose et al., 2013). Based on these findings, a charge dose of 150 C/L was selected for the long term performance experiments as a moderately conservative dose to consistently yield concentrations below 10 μg/L.

4.2. Addressing limitation 1: frequent electrode cleaning is required

4.2.1. Long-term arsenic removal

Fig. 3 shows the arsenic concentration in the filtered sample. All samples shown were collected after receiving a dose of 150 C/L, and are from batches 3-37, excluding 11-13. All sample measurements demonstrate that Fe-EC consistently removed arsenic to below 10 μg/L from the average initial concentration of 153 ± 29.1 μg/L. The average arsenic levels in the samples from the low and high current density reactors were similar, at 1.9 ± 2.1 μg/L and 1.9 ± 2.0 μg/L respectively. Changes in conductivity of raw water (the electrolyte) had no notable impact on

Table 3
Raw water composition during the Field-Experimental (July 2019).

	Cl^- (mg/L)	NO_3^- (mg/L)	SO_4^{2-} (mg/L)	Total alkalinity (as $CaCO_3$) (mg/L)	K (mg/L)	Na (mg/L)	As (μg/L)	P (mg/L)	Ca (mg/L)	Si (mg/L)	Mg (mg/L)	Conductivity (μS/cm)
All data												
Mean	702.8	3.3	644.0	193.2	0.5	584.4	153.2	0.0	15.5	16.4	13.3	2263.6
Standard deviation	519.3	1.0	490.3	25.0	0.3	666.9	29.1	0.1	13.4	0.8	12.5	2111.4
High range												
Mean	1020	3.6	1032.0	211.2	0.8*	1056.0*	184.8	0.1	26.9	15.4	24.2	4585.0
Standard deviation	216.9	1.0	213.2	7.6	N/A	N/A	17.6	ND	4.8	0.6	4.6	790.0
Low range												
Mean	68.4	ND	48.0	162.0	0.3*	112.8*	120.0	ND	2.7	17.0	1.5	441.9
Standard deviation	1.7	ND	3.4	5.1	N/A	N/A	ND	0.1	1.6	0.5	1.6	209.9

The pH values were presented in Table S2. ND ("non-detect") represents values below the detection limits, * These are single measurements.

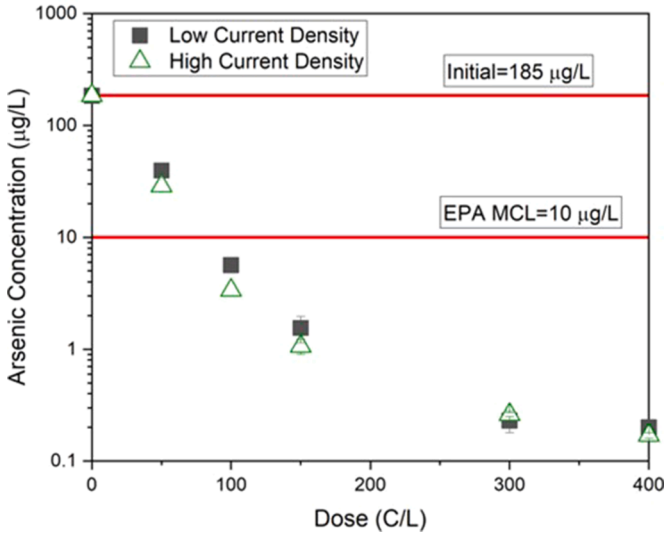

Fig. 2. Arsenic concentration (μg/L) in the filtered samples at various charge dose (Batches number 3-5). Note vertical scale is logarithmic. All data taken in high conductivity period. Data at 0, 50, 100 C/L are duplicate measurements and everything else is triplicate. Standard deviations are indicated by vertical error bars.

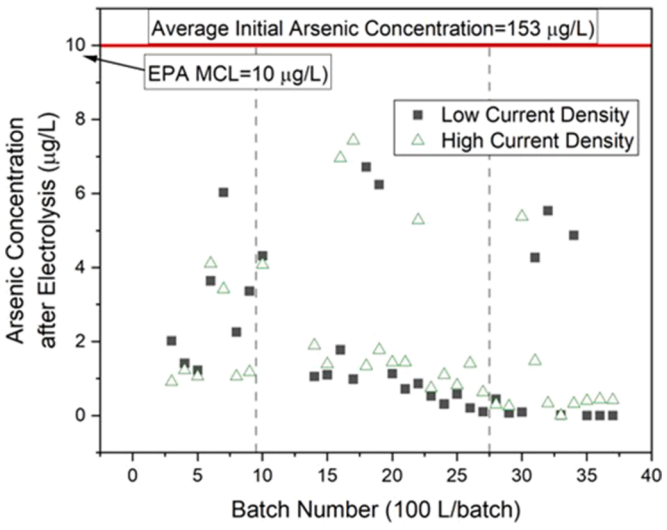

Fig. 3. Arsenic concentration (μg/L) after electrolysis during field trial at 150 C/L (Batch number 3-37). Note linear vertical scale. Batches 11-13 not included in figure as the samples were lost from improper filtration (see text). Two dotted lines demarcate conductivity periods (1-9 and, 28-37 are "high conductivity", and 10-27 is "low conductivity"). The measurement error on each sample point was less than 5% and therefore not shown in the graph for brevity.

arsenic removal.

The electrolyte composition can influence the size and structure of the particles formed in Fe-EC (van Genuchten et al., 2014a). For example, divalent cations (Ca^{2+} and Mg^{2+}) aid in the aggregation of Fe (III) (oxyhyr)oxides, increase the sites available for attachment of As(V) to the precipitates, and increase the size of the particles generated during electrolysis. The average concentrations of Ca and Mg in the groundwater decreased from 26.9 ± 4.8 mg/L and 24.2 ± 4.6 mg/L respectively during the high conductivity period to 2.7 ± 1.6 mg/L and 1.5 ± 1.6 mg/L respectively in the low conductivity period. As a result, when groundwater conductivity was < 1000 μS/cm (or low ionic strength), the 0.45 μm filter failed to remove all of the Fe(III) (oxyhydr) oxide particles, which resulted in high arsenic concentrations in the post-electrolysis filtered (and acid-digested) samples. Thus, arsenic results do not include samples for batches 11-13. After batch 13, when this was realized, instead of collecting the sample after electrolysis we collected samples after the particle separation step in which alum was added. Alum increased the particle size, and allowed for adequate removal of solids by filtration using the 0.45 μm filter. We thereafter obtained correct measurements of the arsenic remaining in solution in the treated water samples. We still do not fully understand the large variance in the measured arsenic values in post-treatment water (all below 10 μg/L, but with a large scatter). Possibly this has to do with the particle separation, which could impact the amount of iron oxides and arsenic going through the 0.45 micron filter into the samples measured for arsenic. This aspect deserves future exploration.

4.2.2. *Faradaic efficiency of total iron*

Fig. 4a presents the Faradaic efficiency of total iron in the beaker scale experiments (see Müller et al., 2019 for Faradaic efficiency calculations). In the low current density reactor, the Faradaic efficiency decreased from about 0.8 to about 0.6 during 16 batch experiments, whereas in the high current density reactor, the Faradaic efficiency remained high (> 85 %) over 16 batch experiments. The results were consistent with prior reported findings. In previous field work, the Faradaic efficiency steadily declined over time in low current density operation (Amrose et al., 2014). In previous lab work, the Faradaic efficiency steadily declined over time in low current density operation and remained relatively high and constant over time in high current density operation (Müller et al., 2019).

However, for experiments conducted in the field using 100 L reactors, unexpected results for Faradaic efficiency were observed. Fig. 4b presents the Faradaic efficiency for the low and high current density

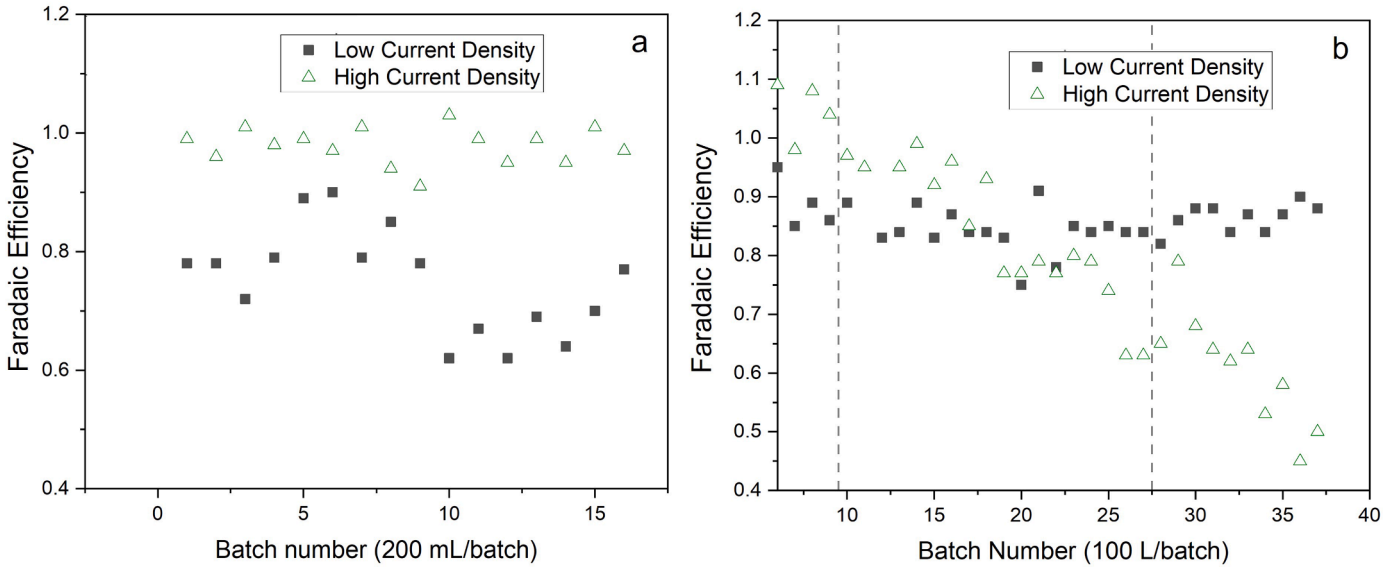

Fig. 4. **a** Faradaic Efficiency in low and high current density experiments at beaker scale using Allensworth farm groundwater that was in the "high" conductivity region. Batches 1-6 were at approximately 196 C/L and batches 7-16 were conducted at approximately 300 C/L. Initial pH was on average 8.29 for all batches. **b** Faradaic Efficiency in low and high current density reactor during field trial (Batches 6-37). Two dotted lines demarcate conductivity regions (1-9, 28-37 is "high" and 10-27 is "low"). Greater than 100% efficiency can be attributed to local regions of nonuniform mixing. The measurement error on each sample point was less than 5% and therefore not shown in the graph for brevity.

reactors for the field trial duration (Batches 3-37). In the field-results from the 100 L low current density reactor, the Faradaic efficiency remained steady at an average value of 86 ± 3.8% over 37 batch experiments. However, in the high current density reactor the Faradaic efficiency steadily decreased, from 109% in B6 to 50% in B37 (greater than 100% efficiency could be attributed to nonuniform mixing). Post-electrolysis, the color of the solution in the high current density reactor steadily became a lighter orange color as the field trial progressed from B6 to B37, consistent with the progressively lower Fe concentrations analytically measured in the solution, as the trial progressed (SI Figure S2). This finding is in contrast with previously published Fe-EC literature (Amrose et al., 2014; Müller et al., 2019) despite having similar operating variables (see Table 1). These results demonstrate that operating Fe-EC at high current density and low charge dosage rate was not beneficial to achieve sustained high Faradaic efficiency over long periods of operation. In the following paragraphs, we discuss various hypotheses and mechanisms to elucidate our findings.

To help understand the sustained Faradaic efficiency in the low current density reactor, we presented indirect measurements such as interface potentials, difference in the weight of the electrodes, and digital images of the electrodes. The interface potential measurements remained constant for a given conductivity period over the duration of the field trial (SI Figure S3) which suggest minimal surface layer (resistive) growth on the electrodes. This hypothesis is further supported by the difference between initial and final weights of the anode plates (1.1 g/plate or ~0.17% of plate weight (see SI Table S3 which presents the change in mass of the electrodes before and after the field trial in the low current density reactor)). One possible hypothesis is that the low concentrations of strongly adsorbing phosphate ions in the groundwater throughout the field trial (Non-Detect ± 0.1 mg/L) could have prevented the growth of surface layers on the electrodes in low current density reactor (van Genuchten et al., 2014a). Another hypothesis is the presence of high levels of dissolved oxygen (post electrolysis, 7.4 ± 0.3 mg/L), which could have prevented the formation of a magnetite surface layer, as seen in other Fe-EC systems (Huang and Zhang, 2005; van Genuchten et al., 2016).

The interface potential measurements could not be taken in the high current density reactor due to the reactor design, which had a pipe and side supports (see items 2 and 3 in SI Figure 11) that prohibited putting anything between the iron plates. The decrease in Faradaic efficiency in the high current density reactor could be due to the non-uniform dissolution of the Fe anode (see Fig. 5) resulting in localized high current density regions to favor other oxidation reactions. One possible mechanism could be due to excessive chloride concentration in the groundwater at our field location; the chloride concentration ranged from 184 mg/L (5 mM as Cl) to 1222 mg/L (34 mM as Cl). Therefore at increasing high current densities with time, the oxidation of Cl^- to Cl_2 could be predominant anodic reaction over Fe(0) to Fe^{2+} oxidation (Wei et al., 2012; Brillas and Martínez-Huitle, 2015; Qian et al., 2019). However, more work is needed to fully elucidate the mechanism and explore the relationship between surface layer formation, water composition, and operating parameters.

To further provide evidence related to the structural integrity and surface layer formation in both high and low current density systems, we provide photographs of electrodes in Fig. 5. For the low current density system, there were 6 cathodes and 6 anodes, and we selected one representative image from each for the table. There are textural differences between the anodes in the high and low current density systems. In the high current density system, the anode has a nonuniform texture which could be due to nonuniform anodic dissolution of the iron electrode, whereas in the low current density system, the anode has a more uniform texture. It is also clear that on both cathodes there is significant light yellow/white surface layer, likely due to calcite precipitation, favored by the higher pH at the cathode. It is important to note on the high current density anode there is a portion on the bottom that is fully consumed by electrolysis. This was expected, as anodes in the system are consumables, and the high current density system had higher cumulative coulombs consumed per electrode surface area. We present Faradaic efficiency versus cumulative coulombs over electrode surface area in SI Figures S4 and S5 to illustrate the difference in coulombs consumed per electrode surface area in each system. These figures demonstrate the Faradaic efficiency as the electrode becomes increasingly consumed. In short-term beaker scale experiments (SI Figure S4), the Faradaic efficiency of total iron decreased with cumulative coulombs per surface area which suggests the surface layer growth on the anode surface at low current density. In contrast, the Faradaic efficiency of total iron remained constant with cumulative coulombs per surface area, likely due to less accumulation of surface layers on the anode surface.

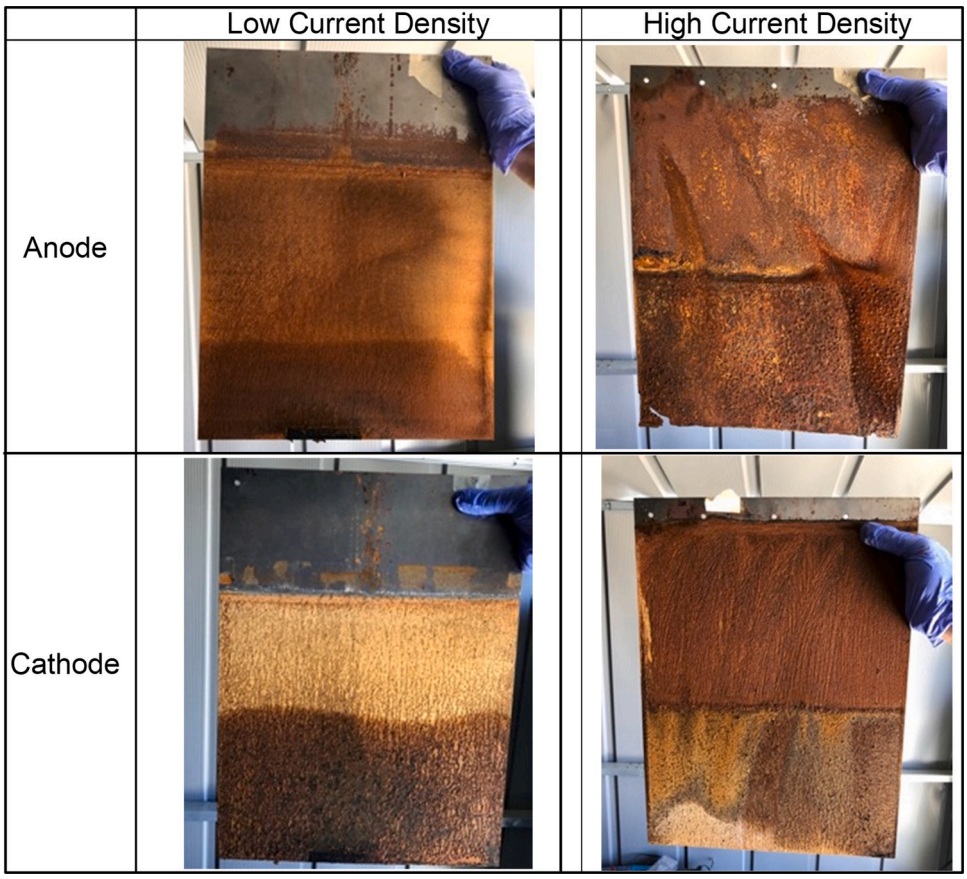

Fig. 5. Digital photographs of electrodes after field trial completion. These images show visually different surface layer growth of the electrodes operated at low current density and high current density. Note that the bottom portions of the electrodes in these images are still wet and may look darker as a result.

However, contrasting results are observed in the field scale Fe-EC system at low and high current densities over long-term operation (Figure S5). In this section, we briefly discussed the possible causes for this contrasting behavior of the Fe-EC system in the field.

4.2.3. Energy intensity and coulombic efficiency of arsenic removal

Energy intensity of arsenic removal (defined as (mWh/L)/(μg arsenic removed/L)) for the high and low current density reactors was calculated to understand the energetic requirements per unit of arsenic removed (SI Figure S6). The energy intensity ranged from 1.5 to 13.6 (mWh/L)/(μg arsenic removed/L) in high current density reactor, which was an order of magnitude higher than the low current density reactor, which ranged from 0.2 to 1.2 (mWh/L)/(μg arsenic removed/L). The order of magnitude increase in energy intensity relative to low current density reactor can be attributed to high operating voltages (greater than 30 V) in the high current density reactor. Current was held constant and arsenic removal remained stable, whereas voltage changed throughout the trial.

The estimated coulombic efficiency of arsenic removal (Coulombs of charge dosed/μg As removed) was similar and consistent across both reactors which suggests that current density did not influence the arsenic removal in Fe-EC (SI Figure S7). This is consistent with the reported findings that the charge dosage rate strongly influences the arsenic removal in the Fe-EC system (Amrose et al., 2013).

4.3. Addressing limitation 2: electrolysis times are long in conventional Fe-EC

Fig. 6 presents the arsenic concentration after electrolysis for varying H_2O_2 concentrations (0, 5, and 26 mg/L H_2O_2) and charge doses (50, 100, and 150 C/L) at a high dosage rate of 30 C/L/min. At 0 mg/L H_2O_2

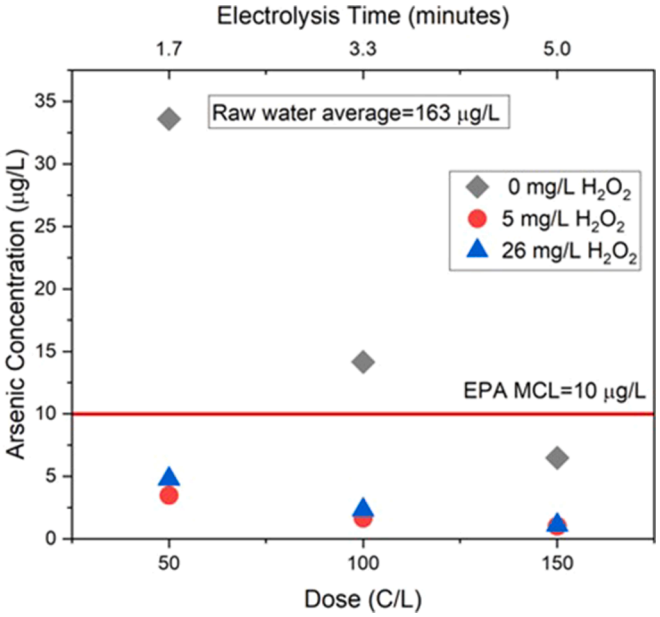

Fig. 6. Arsenic concentration (μg /L) after electrolysis at varying H_2O_2 concentrations (ppm H_2O_2) and Doses (C/L) (C/L=coulombs/liter) at Dosage Rate of 30 C/L/min. The symbol for 0 mg/L H_2O_2 represents a single data point. Those for 5 mg/L and 26 mg/L H_2O_2 are the average of duplicates. Time to complete electrolysis to deliver 50 C/L was 1.7 min, 100 C/L was 3.3 min, and 150 C/L was 5 min. The error bars are not shown because they were smaller than the legends.

(where dissolved oxygen is the primary oxidant), a charge dose of 150 C/L was needed to remove arsenic to below the EPA MCL. The arsenic removal at 150 C/L at high CDR is comparable to the low CDR experiments at low and high current density (see Fig. 3). At 5 mg/L H_2O_2 and 26 mg/L H_2O_2, a charge dose of only 50 C/L was needed to remove arsenic to below the EPA MCL. The time saved in electrolysis when operating at a higher dosage rate, an operating mode enabled by H_2O_2 use, was on the order of hours. Under typical operation of Fe-EC that requires a low dosage rate (Amrose et al., 2013), electrolysis took place over hours, whereas here substantially shorter electrolysis times (1.7 mins) were sufficient to remove arsenic to levels below the MCL. Our results suggest that H_2O_2 combined with a high charge dosage rate rendered Fe-EC a high throughput system while maintaining excellent arsenic removal performance. Iron concentration, Faradaic efficiency, and raw water composition of these experiments are provided in SI Figure S8, SI Figure S9, and SI Table S4 respectively. Faradaic efficiency for these experiments was between 78-92%. Water quality varied throughout the experiment. The conductivity on average was 4630 μS/cm with a standard deviation of 2460 μS/cm.

The energy intensity of arsenic removal (defined earlier) was calculated for (a) traditional Fe-EC operation at low charge dosage rates (SI Figure S6), and (b) novel Fe-EC operation with H_2O_2 injection, at high charge dosage rates (SI Figure S10). Fe-EC operation for removing arsenic with H_2O_2 injection and high charge dosage rates was about as energy intensive as the traditional operation of Fe-EC at low current density (~0.2 (mWh/L)/(μg arsenic removed/L for both). However, the H_2O_2 addition allowed much shorter (more than 40X shorter) electrolysis duration than with traditional Fe-EC. This translates to high throughput of 3600 LPH when H_2O_2 injection was deployed, in contrast to 84 LPH with traditional Fe-EC (low current density reactor).

4.4. *Overcoming limitation 3: waste needs characterization as per California standards*

Solid waste disposal in California requires the waste to pass two different tests, TTLC and STLC. These tests were conducted on dried sludge at a third-party commercial laboratory. Three samples of dried sludge were analyzed. The average results for arsenic were as follows: for TTLC 897 mg arsenic / kg solid-waste, and for STLC 3.6 mg arsenic / liter. The STLC result met the standard for arsenic (allowable maximum is 5 mg/L). The TTLC result was above the standard (allowable maximum is 500 mg/kg), which indicates that the resulting dry sludge contained higher-than-allowable concentration of arsenic. Immobilizing the solid-waste (e.g. by mixing with cement that later hardens into concrete) would be an option to lower the TTLC result to below maximum allowable limit, and certify the final product as non-hazardous waste (Roy et al., 2019). An alternative solution would be to increase the iron dose, decreasing the mass of arsenic per mass of waste.

4.5. *Implications of limitations explored for scale up of Fe-EC in California*

Finally, it is relevant to discuss our results in the context of a (future) scaled up Fe-EC systems implemented for arsenic removal in California. First, while low current density operated under low charge dosage rates was shown to be the best option to maintain Faradaic efficiency under the field conditions, it is not an ideal approach, given its required long duration for electrolysis. Instead, using high dosage rates along with the addition of H_2O_2, would enable short electrolysis times and hence high throughput can be achieved. Further, the use of H_2O_2 might reduce the buildup surface layers and the need for electrode cleaning. However, future research needs to investigate this hypothesis over longer time periods in the field. Hydrogen peroxide is widely available over the counter in the local grocery stores and hardware stores as a household chemical in the United States. It is also widely available for a commercial-scale use at 3% concentration, without requiring hazardous material handling. Larger quantities at higher concentration are also easily available (e.g., 10% or 15%). One Liter of over the counter H_2O_2 (3%) is sufficient to treat nearly 6000 L of arsenic contaminated water at 5 mg/L of H_2O_2 dose in the Fe-EC reactor. Automated dosing pumps can be implemented for in-situ addition of H_2O_2 while filling the reactor tanks before Fe-EC electrolysis. The H_2O_2 supply chain is a minor issue in the United States because commercial delivery services (e.g., FedEX, UPS) transport household chemicals like dilute H_2O_2 on a regular basis to the local stores. The cost of H_2O_2 use is expected to be small and might result in net cost savings. At a concentration tested in the field trial (5 mg H_2O_2/L water), the added cost of H_2O_2 is only $0.004 per L water treated. Use of H_2O_2 would decrease the size of the electrolysis reactor, which would correspondingly decrease fabrication costs and plant footprint. A granular activated carbon filter can be used as a polishing step to remove any residual H_2O_2 before distribution to the community.

5. Conclusions

In this paper, we identified three limitations, and strategies to overcome these limitations, to develop Fe-EC as a technology appropriate for scaling up in the context of arsenic-removal for rural California drinking water. We successfully demonstrated substantially shorter electrolysis time using externally added H_2O_2. We have identified methods by which the waste can be managed in a way which renders it non-hazardous as per California state standards. Finally, we presented the implications of limitations to scale up of Fe-EC in the Californian context to help provide safe drinking water for all. The use of current density to prevent surface layer formation resulted in differing outcomes in the lab and the field (but without undercutting the main findings), and suggests directions for future research in this space.

Declaration of Competing Interest

The authors declare that they have no known competing financial interests or personal relationships that could have appeared to influence the work reported in this paper.

Acknowledgements

We thank our community partners in Allensworth for allowing access to land, and providing raw water, electricity, and their time. We are thankful to the owner of a farm in Allensworth who offered access to a protected fenced-off site, and a concrete pad on the site to build the shed to house the equipment for the field trial. The owner also donated the groundwater and electricity needed for the field trial. We are grateful to several (here un-named) individuals who supported this work through donating their personal funds, and to the following students, faculty, and staff for their support in project formulation, lab work, design, machining, and help with site set up, and field visits: Prof. Isha Ray, Prof. Tom Tomich, Kate Boden, Veena Narashiman, Katie Hendersen, Audrey Gozali, several members of the Gadgil research group, and the staff of the student machine shop at UC Berkeley. We are grateful to two anonymous reviewers of this manuscript; their comments and suggestions have significantly improved this paper.

This research was supported by a National Science Foundation Graduate Research Fellowship, and a National Science Foundation InFEWS fellowship [award number 1633740], both granted to Sara Glade. We are grateful for additional financial support made possible with donations from several individuals, the Rudd Family Foundation Chair funds to Prof. Ashok Gadgil, CERC-WET project supported by the United States Department of Energy at UC Berkeley [award number DE-IA0000018], and award of a TRDRP research grant [grant number T29IR0649] administered by the University of California Office of the President.

Supplementary materials

Supplementary material associated with this article can be found, in the online version, at doi:10.1016/j.watres.2021.117595.

References

Amrose, S., Gadgil, A., Srinivasan, V., Kowolik, K., Muller, M., Huang, J., Kostecki, R., 2013. Arsenic removal from groundwater using iron electrocoagulation: effect of charge dosage rate. J. Environ. Sci. Health Part A 48, 1019–1030. https://doi.org/10.1080/10934529.2013.773215.

Amrose, S.E., Bandaru, S.R.S., Delaire, C., van Genuchten, C.M., Dutta, A., DebSarkar, A., Orr, C., Roy, J., Das, A., Gadgil, A.J., 2014. Electro-chemical arsenic remediation: field trials in West Bengal. Sci. Total Environ. 488–489, 539–546. https://doi.org/10.1016/j.scitotenv.2013.11.074.

Balazs, C.L., Morello-Frosch, R., Hubbard, A.E., Ray, I., 2012. Environmental justice implications of arsenic contamination in California's San Joaquin Valley: a cross-sectional, cluster-design examining exposure and compliance in community drinking water systems. Environ. Health 11. https://doi.org/10.1186/1476-069X-11-84.

Bandaru, S.R., Roy, A., Gadgil, A.J., van Genuchten, C.M., 2020a. Long-term electrode behavior during treatment of arsenic contaminated groundwater by a pilot-scale iron electrocoagulation system. Water Res. 175, 115668 https://doi.org/10.1016/j.watres.2020.115668.

Bandaru, S.R., van Genuchten, C.M., Kumar, A., Glade, S., Hermandez, D., Nahata, M., Gadgil, A., 2020b. Rapid and efficient arsenic removal by iron electrocoagulation enabled with in-situ generation of hydrogen peroxide. Environ. Sci. Technol. https://doi.org/10.1021/acs.est.0c00012.

Barazesh, J.M., Prasse, C., Wenk, J., Berg, S., Remucal, C.K., Sedlak, D.L., 2018. Trace element removal in distributed drinking water treatment systems by cathodic H_2O_2 production and UV photolysis. Environ. Sci. Technol. 52, 195–204. https://doi.org/10.1021/acs.est.7b04396.

Brillas, E., Martínez-Huitle, C.A., 2015. Decontamination of wastewaters containing synthetic organic dyes by electrochemical methods. An updated review. Appl. Catal. B: Environ. 166–167, 603–643. https://doi.org/10.1016/j.apcatb.2014.11.016.

California Code of Regulations, 2021. Characteristic of Toxicity [WWW Document]. URL https://govt.westlaw.com/calregs/Document/I07DBE58C0F8C446C9715168D2C88CC9E?viewType=FullText&originationContext=documenttoc&transitionType=StatuteNavigator&contextData=%28sc.Default%29 (accessed 5.31.21).

Colby, E.J.H., Young, T.M., Green, P.G., Darby, J.L., 2010. Costs of arsenic treatment for potable water in California and comparison to United States environmental protection agency affordability metrics. JAWRA J. Am. Water Resour. Assoc. 46, 1238–1254. https://doi.org/10.1111/j.1752-1688.2010.00488.x.

Delaire, C., Amrose, S., Zhang, M., Hake, J., Gadgil, A., 2017. How do operating conditions affect As(III) removal by iron electrocoagulation? Water Res. 112, 185–194. https://doi.org/10.1016/j.watres.2017.01.030.

Dubrawski, K.L., van Genuchten, C.M., Delaire, C., Amrose, S.E., Gadgil, A.J., Mohseni, M., 2015. Production and transformation of mixed-valent nanoparticles generated by Fe(0) electrocoagulation. Environ. Sci. Technol. 49, 2171–2179. https://doi.org/10.1021/es505059d.

Gadgil, A., 2018. Personal communication with Ashok Gadgil by Livpure officers.

Hernandez, D., Boden, K., Paul, P., Bandaru, S., Mypati, S., Roy, A., Amrose, S., Roy, J., Gadgil, A., 2019. Strategies for successful field deployment in a resource-poor region: arsenic remediation technology for drinking water. Dev. Eng. 4 https://doi.org/10.1016/j.deveng.2019.100045.

Huang, Y.H., Zhang, T.C., 2005. Effects of dissolved oxygen on formation of corrosion products and concomitant oxygen and nitrate reduction in zero-valent iron systems with or without aqueous Fe2+. Water Res. 39, 1751–1760. https://doi.org/10.1016/j.watres.2005.03.002.

Hug, S.J., Leupin, O., 2003. Iron-catalyzed oxidation of arsenic(III) by oxygen and by hydrogen peroxide: pH-dependent formation of oxidants in the fenton reaction. Environ. Sci. Technol. 37, 2734–2742. https://doi.org/10.1021/es026208x.

King, D.W., Farlow, R., 2000. Role of carbonate speciation on the oxidation of Fe(II) by H2O2. Mar. Chem. 70, 201–209. https://doi.org/10.1016/S0304-4203(00)00026-8.

Lakshmanan, D., Clifford, D.A., Samanta, G., 2010. Comparative study of arsenic removal by iron using electrocoagulation and chemical coagulation. Water Res., Groundwater Arsenic: From Genesis Sustain. Remediation 44, 5641–5652. https://doi.org/10.1016/j.watres.2010.06.018.

Li, L., van Genuchten, C.M., Addy, S.E.A., Yao, J., Gao, N., Gadgil, A.J., 2012. Modeling As(III) oxidation and removal with iron electrocoagulation in groundwater. Environmental Science and Technology 46 (21), 12038–12045. https://doi.org/10.1016/j.watres.2017.01.030.

Müller, S., Behrends, T., van Genuchten, C.M., 2019. Sustaining efficient production of aqueous iron during repeated operation of Fe(0)-electrocoagulation. Water Res. 155, 455–464. https://doi.org/10.1016/j.watres.2018.11.060.

Qian, A., Yuan, S., Xie, S., Tong, M., Zhang, P., Zheng, Y., 2019. Oxidizing capacity of iron electrocoagulation systems for refractory organic contaminant transformation. Environ. Sci. Technol. 53, 12629–12638. https://doi.org/10.1021/acs.est.9b03754.

Ratna Kumar, P., Chaudhari, S., Khilar, K.C., Mahajan, S.P., 2004. Removal of arsenic from water by electrocoagulation. Chemosphere 55, 1245–1252. https://doi.org/10.1016/j.chemosphere.2003.12.025.

Roy, A., van Genuchten, C.M., Mookherjeec, I., Debsarkara, A., Duttaa, A., 2019. Concrete stabilization of arsenic-bearing iron sludge generated from an electrochemical arsenic remediation plant. J. Environ. Manage. 233, 141–150. https://doi.org/10.1016/j.jenvman.2018.11.062.

State Water Resources Control Board, 2018. Secondary drinking water standards.

State Water Resources Control Board, 2015. Safe drinking water plan for California: state water resources control board report to the legislature in compliance with health & safety code section 116365.

State Water Resources Control Board, 2013. Communities that rely on a contaminated groundwater source for drinking water. State Water Resour. Control Board.

State Water Resources Control Board, 2021 n.d. GAMA groundwater information system [WWW Document]. URL https://gamagroundwater.waterboards.ca.gov/gama/gamamap/public/Default.asp (accessed 1.31.20).

United States Environmental Protection Agency, 2021 n.d. National primary drinking water regulations [WWW Document]. United States EPA. URL https://www.epa.gov/ground-water-and-drinking-water/national-primary-drinking-water-regulations (accessed 12.11.17).

United States Congress, 2019. Safe drinking water act-(Title XIV of public health service act).

van Genuchten, C.M., Bandaru, S.R.S., Surorova, E., Amrose, S.E., Gadgil, A.J., Peña, J., 2016. Formation of macroscopic surface layers on Fe(0) electrocoagulation electrodes during an extended field trial of arsenic treatment. Chemosphere 153, 270–279. https://doi.org/10.1016/j.chemosphere.2016.03.027.

van Genuchten, C.M., Gadgil, A.J., Peña, J., 2014a. Fe(III) nucleation in the presence of bivalent cations and oxyanions leads to subnanoscale 7 Å polymers. Environ. Sci. Technol. 48, 11828–11836. https://doi.org/10.1021/es503281a.

van Genuchten, C.M., Peña, J., Amrose, S.E., Gadgil, A.J., 2014b. Structure of Fe(III) precipitates generated by the electrolytic dissolution of Fe(0) in the presence of groundwater ions. Geochim. Cosmochim. Acta 127, 285–304. https://doi.org/10.1016/j.gca.2013.11.044.

Wan, W., Pepping, T.J., Banerji, T., Chaudhari, S., Giammar, D.E., 2011. Effects of water chemistry on arsenic removal from drinking water by electrocoagulation. Water Res. 45, 384–392. https://doi.org/10.1016/j.watres.2010.08.016.

Wang, L., Chen, A.S., Sorg, T.J., Supply, W., 2011. Costs of arsenic removal technologies for small water systems: United States EPA arsenic removal technology demonstration program. Powell, OH.

Wei, M.-C., Wang, K.-S., Huang, C.-L., Chiang, C.-W., Chang, T.-J., Lee, S.-S., Chang, S.-H., 2012. Improvement of textile dye removal by electrocoagulation with low-cost steel wool cathode reactor. Chem. Eng. J. 192, 37–44. https://doi.org/10.1016/j.cej.2012.03.086.

Welch, A.H., Westjohn, D.B., Helsel, D.R., Wanty, R.B., 2000. Arsenic in ground water of the United States: occurrence and geochemistry. Groundwater 38, 589–604. https://doi.org/10.1111/j.1745-6584.2000.tb00251.x.

World Health Organization, 2017. Arsenic [WWW Document]. WHO. URL http://www.who.int/mediacentre/factsheets/fs372/en/ (accessed 2.23.18).